

1 **Potentialities of biotechnological recovery of hydrogen and short- and medium-**  
2 **chain organic acids from the co-fermentation of cheese whey and Yerba Mate (*Ilex***  
3 ***paraguariensis*) waste**

4 Antônio Djalma Nunes Ferraz Júnior <sup>a</sup>, Laura Fuentes <sup>a</sup>, Victoria de la Sovera <sup>a</sup>, Patricia  
5 Bovio-Winkler <sup>a</sup>, Felipe Eng <sup>a,b</sup>, Mariángeles Garcia <sup>a</sup>, Claudia Etchebehere <sup>a</sup>

6 <sup>a</sup> Laboratorio de Ecología Microbiana, Bioquímica y Genómica Microbiana, Instituto de Investigaciones  
7 Biológicas “Clemente Estable”. Av. Italia 3318, Montevideo, Uruguay.

8  
9 <sup>b</sup> Laboratório de Processos Biológicos, Escola de Engenharia de São Carlos, Universidade de São Paulo  
10 (LPB/EESC/USP). Av. João Dagnone 1100 - Santa Angelina, 13563-120, São Carlos, SP, Brasil.

11  
12 \* Correspondence to: Claudia Etchebehere, Microbial Ecology Laboratory, Clemente Estable Biological  
13 Research Institute, Ministry of Education, Av. Italia 3318, Montevideo, Uruguay; phone: (+598)  
14 24871616; fax: (+598) 24875461; E-mail: [cetchebehere@iibce.edu.uy](mailto:cetchebehere@iibce.edu.uy); Webpage: [www.iibce.edu.uy](http://www.iibce.edu.uy)

15

16

17

18

19

20

21 **Highlights**

- 22 • Co-fermentation improved hydrogen production in up 7.5-folds compared to the  
23 sole CW-fed system.
- 24 • The initial pH had no effect on hydrogen-producing batch reactors.
- 25 • Hydrogen was produced as a coproduct to butyrate.
- 26 • Design of experiment indicated operating conditions to the production of lactate  
27 and caproate.

28

29

30

31

32

33

34

35

36

- 1 **List of abbreviation**
- 2  $b_1$  - linear coefficients for the YMW concentration
- 3  $b_2$  - linear coefficients for pH
- 4  $b_3$  - linear coefficients for the inoculum concentration
- 5 CCD - Central Composite Designs
- 6 CW - Cheese Whey
- 7 DNS - 3,5-Dinitrosalicylic acid method
- 8 DoE - Design of Experiments
- 9 F/M - Food-to-Microorganisms ratio
- 10  $H_2Y$  - Hydrogen Yield
- 11 HTS - High-Throughput Sequencing
- 12 PCA - Principal Component Analysis
- 13 RBO - Reverse  $\beta$ -Oxidation
- 14 RSM - Response Surface Methodology
- 15 SCOD - Soluble Chemical Demand of Oxygen
- 16 TCOD - Total Chemical Demand of Oxygen
- 17 TRS - Total Reducing Sugars
- 18 TS - Total solids
- 19 TVS - Total Volatile Solids
- 20  $X_1$  - YMW concentration
- 21  $X_{12}$  - coefficients for the interaction between YMW concentration and pH
- 22  $X_{13}$  - coefficients for the interaction between YMW concentration and inoculum
- 23 concentration
- 24  $X_2$  - pH
- 25  $X_{23}$  - coefficients for the interaction between pH and inoculum concentration
- 26  $X_3$  - inoculum concentration
- 27 Y - Experimental Response
- 28  $\hat{Y}$  - Predicted Response
- 29 YMW - Yerba Mate Waste
- 30

1 **Abstract**

2 Co-fermentation of cheese whey (CW) and thermal-alkaline pre-treated Yerba Mate  
3 (*Ilex paraguariensis*) waste (YMW) was performed aiming to produce biohydrogen  
4 and/or short- and medium-chain organic acids. Central Composite Designs (CCD) was  
5 chosen as the experimental design for evaluating the combinations of three independent  
6 variables namely YMW concentration, pH and inoculum concentration in hydrogen  
7 yield ( $H_2Y$ ; response variable). The increase of inoculum and YMW concentrations had  
8 positive effect in biohydrogen production and yield ( $H_2Y_{max}$  of  $1.35 \text{ mMH}_2\text{g}^{-1} \text{ VS}_{added}$ )  
9 whereas the initial pH had no significant effect on it. Hydrogen was produced as a  
10 coproduct to butyrate mainly. Acetate from homoacetogenesis was accounted in all  
11 conditions evaluated. The CCD also indicated operating conditions to produce  
12 moderate-to-high concentrations of short and medium-chain organic acids such as  
13 butyrate (~135 mM), caproate (~45 mM) and lactate (~140 mM). 16S rRNA gene  
14 sequences analysis revealed five groups of microorganisms related to hydrogen, lactate  
15 and caproate production, ethanol-hydrogen co-production and hydrogen consumption.

16

17

18

19

20

21

22

23

24

25

26

27

28

29

30 **Keywords:** Central Composite Design; Response Surface Methodology; Butyrate-type  
31 fermentation, Caproate-type fermentation, Lactate-type fermentation.

## 1        **1. Introduction**

2        Fermentation is one the first steps of residues decomposition by microorganisms. In this  
3        step, hydrogen is the most desired coproduct for being a versatile energy carrier used for  
4        fossil fuel refining and production of chemicals, including biofuels (IEA, 2019). Other  
5        coproducts of industrial interests such as short- and medium-chain organic acids,  
6        alcohols and solvents can also be obtained through fermentation process which makes it  
7        an ideal multipurpose technology (Borin et al., 2019; Luongo et al., 2019; Mota et al.,  
8        2018).

9        In general terms, fermentation technology comprises a cascade of reactions which are  
10       primarily related to the production and consumption of hydrogen, considering a  
11       fermentative system using non-sterile mixed cultures (Levin et al., 2004). In that case,  
12       high production of hydrogen is associated to the mixture of acetate and butyrate  
13       fermentation route end-products whilst its low production is associated to other reduced  
14       end-products such as acetone, butanol, ethanol and lactate (Ferraz Júnior, 2013).  
15       Finally, hydrogen consumption is reported in methanogenesis and homoacetogenesis  
16       routes. These reactions will be reported in depth in *section 3.6*.

17       The success of fermentative systems is allied to multiple factors (substrate-type,  
18       temperature, pH, inoculum, regime operation) which are interrelated (Akhlaghi et al.,  
19       2017; Koyama et al., 2016). The operating pH (controlled along the process) is an  
20       important individual-factor in fermentative systems. It indicates the hydrolysis and  
21       fermentation degree; determines the activity of hydrogenase and the metabolic routes  
22       (Kim et al., 2011). Extreme high pH values can negatively affect the activity  
23       of hydrogen-producing microorganisms as well as extreme low pH values can result in  
24       inhibition of the hydrogenase activity (Mohd Yasin et al., 2011) diverting the  
25       corresponded pathways to the production of solvents (i.e., alcohols) (Fuess et al., 2018).  
26       Similarly, the relative concentration of active biomass (inoculum) in the system and the  
27       substrate available to be consumed is expressed as food-to-microorganisms (F/M) ratio.  
28       This ratio can shift from substrate-limited to substrate-sufficient growth but also to  
29       substrate-excess unbalancing the anabolic and catabolic reactions and, thus, affecting  
30       the yield of substrate conversion into by-products (Akhlaghi et al., 2017; Liu, 1996).

31       Different wastes and wastewaters have been used as feedstock in fermentative systems  
32       including agricultural and food industry wastewater, lignocellulosic biomass and

1 organic fraction of municipal solid waste (Castelló et al., 2020). However, some  
2 feedstock can present undesirable features or even a nutritional deficit which may affect  
3 the process to proceed properly. For instance, algal biomass has been adopted as the  
4 main carbon source for sewage sludge fermentation in order to dilute the inherent  
5 inhibitors to the latter residue (Yin et al., 2021). Similarly, rich-protein substrate  
6 (microalgae) and rich-carbohydrate substrate (macroalgae and rice residues) have been  
7 used as mixed substrate to achieve better ratios of carbon-nitrogen and improve the  
8 performance of fermentative organic acids and hydrogen production (Sun et al., 2018;  
9 Xia et al., 2016). The simultaneous fermentation of two or more residues, also known as  
10 co-fermentation, might represent an alternative to mitigate the aforementioned  
11 drawbacks (Grosser and Neczaj, 2018; Yang et al., 2019) and increase the production of  
12 target products.

13 Cheese whey (CW) is a residual nutrient-rich liquid stream from dairies industries that  
14 has been extensively studied to fermentative purposes (Basak et al., 2018; Lovato et al.,  
15 2018; Rao and Basak, 2021). However, hydrogen production instability and process  
16 inhibition by accumulation of organic acids have been reported and attributed to its lack  
17 of alkalinity (low pH) and high organic matter concentration, respectively (Fernández et  
18 al., 2014; Lovato et al., 2018, Lovato et al., 2021).

19 Yerba Mate (*Ilex paraguariensis*) waste (YMW) is one the most important  
20 lignocellulosic residue in Southern Cone of Latin America (Argentina, Brazil, Chile,  
21 Paraguay, and Uruguay) and after its thermal-alkaline pretreatment might be a co-  
22 substrate for CW fermentation able to increase bioproducts production. The thermal-  
23 alkaline pretreated YMW presents a high pH ( $13.1 \pm 0.6$ ) (Ferraz Júnior et al., 2020)  
24 and might be able to “buffer” the system by increasing the pH to suitable values of  
25 fermentative process without additional costs with alkalis.

26 Co-fermentation of CW and YMW for biohydrogen and/or short- and medium-chain  
27 organic acids production has not been described in any literature before, therefore, it  
28 represents a novelty and the aim of this study. The design of experiments (DoE) was  
29 used as a systematic method to investigate fundamentals factors of the process (initial  
30 pH, concentration of inoculum and YMW) in batch-mode to attain the production of  
31 hydrogen and/or short- and medium- chain organic acids. High-throughput sequencing  
32 (HTS) technology was also performed to assess the microbial community dominant in  
33 the co-fermenting system.



1 Equation 3 was used to decode  $\alpha$  value to access the experimental values of the  
2 variables to be studied.

$$3 \quad \alpha = \frac{z_i - \bar{z}}{\frac{\Delta z}{2}} \quad (3)$$

4 Where  $\alpha$  is the coded value of axial point,  $z_i$  is the experimental value of the level,  $\bar{z}$  is  
5 the average between the lower (-) and higher (+) value of the level which is exactly the  
6 value of level zero (0) and  $\Delta z$  is the difference between the lower (-) and higher (+).

7 The coefficients were obtained using the method of least squares. Linear models were  
8 used to evaluate the influence of all the experimental variables of interest and the  
9 interaction effects on the response, according to Equation 4.

$$10 \quad Y = b_0 + b_1 X_1 + b_2 X_2 + b_3 X_3 + b_{12} X_1 X_2 + b_{13} X_1 X_3 + b_{23} X_2 X_3 + e \quad (4)$$

11 Where Y is the predicted response (hydrogen yield – H<sub>2</sub>Y, in MmH<sub>2</sub>.g<sup>-1</sup> VS<sub>added</sub>); b<sub>0</sub> is a  
12 constant (average value average of all observations); b<sub>1</sub>, b<sub>2</sub> and b<sub>3</sub> are the linear  
13 coefficients for the dependent variables (X<sub>1</sub>, X<sub>2</sub> and X<sub>3</sub>, respectively); X<sub>1</sub>, X<sub>2</sub> and X<sub>3</sub> are  
14 the variables (YMW concentration, pH and inoculum concentration, respectively); b<sub>12</sub>,  
15 b<sub>13</sub> and b<sub>23</sub>, are the coefficients for the interactions X<sub>12</sub>, X<sub>13</sub> and X<sub>23</sub>, respectively; and e  
16 is the random error associated with the model.

17 The evaluation of significant effects and coefficients was based on statistical decision  
18 using analysis of variance (ANOVA) and the Student's distribution with p-value of 0.05.  
19 The significant factors were selected and a response surface methodology (RSM) was  
20 used to predict the optimal region on the surface defined by the factors. In this case, the  
21 best values of the variables able to produce the higher amount of biohydrogen.

22 **[Table 2]**

23

#### 24 **2.4. Co-fermentation process of CW and YMW (batch mode)**

25 Co-fermentation of CW and YMW was performed in batch mode. The experiments  
26 were performed in parallel according to Table 2. The mixture of feedstocks was  
27 performed at room temperature (20-22°C). Schott bottles (DURAN<sup>®</sup> containing a total  
28 volume of 500 mL) were flushed with nitrogen gas, sealed with butyl rubber stoppers,  
29 and incubated at 37 °C until hydrogen production ceased. Continuous stirring was kept  
30 at 150 rpm. The reaction volume was 200 mL. The pH of all experiments was not  
31 controlled during co-fermentation process. Accumulated hydrogen production was

1 measured with a gas volume meter (AMPTS II from Bioprocess Control) previously  
2 washed in NaOH solution (12% w/v). Gas production is expressed at standard  
3 temperature (0 °C), pressure (1 atm), and zero water–vapor pressure.

#### 4 **2.5. Chemical analysis**

5 The pH value was measured by using a pH meter (OAKTON pH 11 series). Total  
6 reducing sugars (TRS) were determined using the 3,5-dinitrosalicylic acid (DNS)  
7 method (Miller, 1959). Chemical Demand of Oxygen (COD), total solids (TS) and total  
8 volatile solids (TVS) were determined according to APHA (2005). Organic acids (C2-  
9 C6) were determined by Gas Chromatography equipped with a Flame Ionization  
10 Detector (GC/FID) (Adorno et al., 2014). Lactic acid was determined by spectrometry  
11 according to Borshchevskaya et al. (Borshchevskaya et al., 2016). Hydrogen (H<sub>2</sub>),  
12 Carbon dioxide (CO<sub>2</sub>) and methane (CH<sub>4</sub>) were measured using a gas chromatograph  
13 (GC-2014, Shimadzu), equipped with a thermal conductivity detector. A packed column  
14 was used with the following dimensions 2 m × 1 mm × 1/16 inch. Temperatures of the  
15 injection port and the detector were 120 °C. The initial temperature of the oven was 30  
16 °C, and the final temperature of the column was 110 °C with a temperature increase of  
17 35 °C/min. Ar was used as a carrier gas with a pressure of 8 bar.

#### 18 **2.6. DNA extraction, PCR amplification and High-Throughput Sequencing** 19 **(HTS) of co-fermentation systems samples**

20 Biomass samples were collected from each batch reactor at the end of its operation.  
21 However, a composed sample (1:1:1) was generated for the “S.no.” 9, 10 and 11  
22 (replication). 10 mL of samples were centrifuge to separate the biomass (3,000 rpm, 10  
23 min) and genomic DNA was extracted with the ZR Soil Microbe DNA MiniPrep™ kit  
24 (Zymo Research) following the manufacturer’s instructions. DNA encoding the 16S  
25 rRNA gene was amplified by PCR with primers for the bacteria domain: 520F (5-  
26 AYTGGGYDTAAAGNG-3') and 802R (TACNNGGGTATCTAATCC) (Claesson et  
27 al., 2009). Barcodes (10 bp) were added to the amplified 16S rRNA in order to identify  
28 the samples after sequencing. The reaction was performed using 1.5 µl of amplified  
29 16S rRNA, 0.5 µl of primers and 12.5 µl of buffer ranger mix (1.5 mM) for a final  
30 reaction volume of 25 µl per sample. The conditions were as follow: initial denaturation  
31 (95°C for 5 min), 35 cycles of denaturation (94°C for 30 s), hybridization (55°C for 30  
32 s), extension (72°C for 1 min) and final extension (72°C at 10 min). The tagged



1 amplification was purified using the Zymoclean™ Gel DNA Recovery kit following the  
2 manufacturer's protocol. The purified products (tagged amplicons) were sequenced by  
3 Ion Torrent PGM technology at Biological Research Institute “Clemente Estable”,  
4 Montevideo, Uruguay. The raw reads generated were processed using QIIME software  
5 version 1.9.1 (Caporaso et al., 2012, 2011). Low quality reads (coefficient greater than  
6 25) were filtered, trimmed primers, adapters, and barcodes, and reads less than 200  
7 bases in length were eliminated. Chimeras and noise in the sequencing reads were  
8 removed leaving high quality reads for the samples. Sequences were clustered into  
9 operational taxonomic units (OTU) using UClust algorithm (Edgar et al., 2011), based  
10 on the 97% identity threshold (de novo-based OTU picking strategy). OTUs represented  
11 by one sequence (singletons) were removed from the analysis. Silva database (version  
12 132) was used for the taxonomic classification of the readings with a confidence  
13 threshold of 80%. The raw data was deposited at National Center for Biotechnology  
14 Information (NCBI) under accessing number: [PRJNA684595](https://www.ncbi.nlm.nih.gov/submit/PRJNA684595).

## 15 **2.7. Calculations and kinetics analysis**

16 The volume of substrate, co-substrate, inoculum and the food/microorganism ratio  
17 (F/M) were calculated based on the following system of equations (6) and (7):

$$18 \quad V_w = V_s + V_{CS} + V_I + V_h \quad (6)$$

19 Where,  $V_t$  is the working or reactional volume (mL),  $V_s$  is the substrate volume (mL),  
20  $V_{CS}$  is the co-substrate volume (mL),  $V_I$  is the volume of inoculum (mL) and  $V_h$  is the  
21 volume of headspace.

$$22 \quad F/M = \frac{(V_s + V_{CS}) \cdot COD_i}{V_I \cdot TVS_I} \quad (7)$$

23 Where, F/M is commonly given in  $\text{g-COD} \cdot \text{g}^{-1} \text{TVS}$  although is expressed as  
24  $\text{g-O}_2 \cdot \text{L}^{-1}$ .  $COD_i$  is the initial COD,  $TVS_I$  is the total volatile solids of inoculum, in  $\text{g-}$   
25  $\text{TVS} \cdot \text{kg}^{-1}$ . The dry apparent specific weight ( $\gamma_d$ ) assumed was  $600 \text{ kg} \cdot \text{m}^3$ .

26 The experimental data from the optimum condition (Section 2.4) was adjusted to the  
27 modified Gompertz equation (GM) using the software package Statistica® 8.0 in order  
28 to evaluate the kinetics of the co-fermentation process (Equation 8).

$$29 \quad P = AcH_2P \cdot \exp \left\{ - \exp \left[ \frac{R \cdot e}{P} \cdot (\lambda - t) + 1 \right] \right\}$$

30 (8)

1 Where,  $AcH_2P$  is cumulative hydrogen production expressed in mM,  $\lambda$  is lag-phase  
2 time in d, P is hydrogen production potential also in mL, R is the hydrogen production  
3 rate in  $mM \cdot d^{-1}$  and  $e$  is  $\exp(1)$  (i.e., Euler number: 2.71828).

4 The theoretical expected hydrogen production and the acetate produced from  
5 homoacetogenesis were calculated using Equations (9) and (10) as presented in Ferraz  
6 Júnior et al., 2020.

$$7 \quad H_{2 \text{ theoretical}} = 2[A] + 2[B] - [P] \quad (9)$$

$$8 \quad Acetate_{\text{homoacetogenesis}} = \frac{2[A] + 2[B] - [P] - [H_2]}{6} \quad (10)$$

9 Where, [A], [B], [P] and [H<sub>2</sub>] are the measured acetic, butyric and propionic acids, and  
10 the hydrogen concentrations in mM, respectively.

11 Principal component analysis (PCA) was performed using STATISCA 10 previously  
12 described in (Ferraz Júnior et al., 2020).

### 13 **3. Results and discussion**

#### 14 **3.1. Hydrogen yield: variable response**

15 Full factorial CCD was employed to determine the individual and interactive effects of  
16 thermal-alkaline pretreated Yerba Mate (*Ilex paraguariensis*) waste concentration  
17 (YMW, % w/w), pH and inoculum concentration (% w/w) on the co-fermentation  
18 process which presented cheese whey (CW) as the main substrate. Table 3 presents the  
19 experimental (Y) and predicted response ( $\hat{Y}$ ) expressed as hydrogen yield (H<sub>2</sub>Y).

#### 20 **[Table 3]**

21 The different conditions evaluated had a strong influence on hydrogen yield. The  
22 highest H<sub>2</sub>Y (1.35  $mMH_2 \cdot g^{-1} VS_{\text{added}}$ ) were obtained when the concentration of YMW  
23 and inoculum were at their higher levels and the pH at its lower. In contrast, the lowest  
24 corresponding value (H<sub>2</sub>Y; 0.31  $mMH_2 \cdot g^{-1} VS_{\text{added}}$ ) were achieved in absence of YMW  
25 and at the lowest concentration of inoculum, indicating that the co-fermentation process  
26 was able to increase biohydrogen outputs.

27 The maximum H<sub>2</sub>Y obtained in the CCD experiments is comparable with data found by  
28 other researchers (Table 4). Lee et al., (2008) reported much lower H<sub>2</sub>Y (0.44  $mMH_2 \cdot g^{-1}$   
29  $VS_{\text{added}}$ ) in batch reactors fed with kitchen vegetable wastes. In another study, Dareioti

1 et al., (2014) observed a  $H_2Y$  of  $1.06 \square MmH_2.g^{-1} VS_{added}$  from the co-fermentation  
2 process of olive mill wastewater, cheese whey and cow manure. In turn, Lucas et al.,  
3 (2015) evaluated the potential to produce hydrogen from cassava starch, dairy and citrus  
4 wastes reaching  $H_2Y$  value of  $1.27 \square MmH_2.g^{-1} VS_{added}$  which is similar to the obtained  
5 in this study. Exceptionally, Marone et al., (2015) and Basak et al., (2018) reported  $H_2Y$   
6 values four-times higher ( $4.98-5.69 MmH_2.g^{-1} VS_{added}$ , respectively) than the maximum  
7 value observed in this study. The mentioned authors performed an optimization of  
8 substrate composition and kinetics studies for hydrogen production from the co-  
9 fermentation of agro-industrial residues with cheese whey as common substrate.

10 **[Table 4]**

11 In terms of hydrogen production, there is no clear set condition for maximizing it,  
12 especially regarding the initial pH (uncontrolled pH) that has been reported at values of  
13 5.5 and 7.0. This range is way further concerning lactate (5.5 – 11.0) and caproate (5.5 –  
14 8.5) production. In this sense, the fermentation process might be individually optimized  
15 via a careful balancing of the different operating conditions, regardless the feedstock,  
16 type of reactor and feed mode used (Table 4).

17 **3.2.Co-fermentation process conditions: validation of model, significant effects,**  
18 **and coefficients interactions**

19 Linear model with interaction among variables (Equation 4) was performed in order to  
20 find out the relationship between responses and process variables of co-fermentation  
21 process (Table 5). Most of the total response variation around the mean value ( $b_0$ ) was  
22 explained by the regression equation (Regression *p-value* significative at 5% level) and  
23 the remainder left as residual (Residual *p-value* not significance at 5% level).  
24 Furthermore, the model was found to be accurate ( $R^2$  of 0.72) indicating that more than  
25 70% of the observed values could be explained by the model. The same model was used  
26 to explain the effect of variables on four alkaline pre-treatments of YMW (Ferraz-  
27 Júnior, 2020). The authors' reported slightly higher values of  $R^2$  ( $\geq 0.89$ ) than what was  
28 found in this study. This may be due to axial points not being considered in the model,  
29 indicating the variable response values were closer to the central point (i.e., greater  
30 control of casual variability) but with lower range responses.

31

1 **[Table 5]**

2 The factors  $X_1$  (YMW concentration) and  $X_3$  (inoculum concentration) at the levels  
3 studied are significant, indicating that they might be fixed at the lowest value when  
4 evaluated individually. Interestingly, the factor  $X_2$  (initial pH, *i.e.*, non-controlled pH)  
5 had no influence on the co-fermentation process, suggesting that it can be fixed at any  
6 value between the two levels. Furthermore, the final pH measured from each batch  
7 reactor was between 3.4 and 5.2 regardless of its initial value, indicating that the  
8 fermentation products were able to decrease the pH even from its highest level (S. no.  
9 15; pH of 12.7 – Table 2). This finding is also corroborated by Koyama et al., (2016)  
10 who potentially computed the use of industrial effluent in hydrogen-producing systems  
11 at its original pH (4.8). Hydrogen production under extreme conditions of pH (2.8 and  
12 10.0) were also reported by Mota et al., (2018) and Li et al., (2020), therefore, being  
13 consistent with the current result.

14 Interaction between factors are important for process optimization (Ferraz Júnior et al.,  
15 2020). The individual interaction  $X_1X_2$  (YMW concentration and pH) and  
16  $X_1X_3$  (concentration of YMW and inoculum) were significant. Additionally, the  $X_1X_3$   
17 interaction had the strongest effect on the process and according to this finding, both  
18 variables should be studied at their highest levels for a greater response. The best level  
19 of independent variables and their interactions on the co-fermentation process was then  
20 evaluated with a response surface plot (Figure 1).

21 **[Figure 1]**

22 By applying linear regression analysis to the experimental results, Equation 11 was  
23 obtained to describe the co-fermentation process of cheese whey and Yerba Mate waste  
24 using the uncoded independent variables.

25 
$$H_2Y = -0.002*(YMW)^2 - 0.001*(Inoculum)^2 + 0.080*(YMW) + 0.088*(Inoculum) -$$
  
26 0.655 (Equation 11)

27 In the case,  $H_2Y$  is the hydrogen yield in  $MmH_2.g^{-1} VS_{added}$ , YMW is the concentration  
28 of Yerba Mate in % and Inoculum is the concentration of sludge added to the reactor  
29 also in %.

30 **3.4. Effects of food to microorganisms (F/M) ratios**

1 Different ratios of F/M on hydrogen production from the co-fermentation of CW and  
2 YMW were evaluated based on the CCD experiments. The different volumes of  
3 mixtures between CW, YWM and inoculum in the batch reactors resulted in F/M ratios  
4 of 1.5, 1.8, 2.3, 2.6, 3.6, 5.6 and 9.5  $\text{g COD} \cdot \text{g}^{-1} \text{vs}$ . The highest and lowest values of  $\text{H}_2\text{Y}$   
5 of co-fermentation process were archived at F/M ratio of 2.3 and 9.5  $\text{g COD} \cdot \text{g}^{-1} \text{vs}$ ,  
6 respectively, demonstrating the need for high amounts of inoculum (~ 20% w/v) able to  
7 convert complex substrates such as lignocellulosic materials in hydrogen. Similar values  
8 were observed by Nasr et al. (2011) using thin stillage as substrate. By contrast, higher  
9 ratios of F/M (10.6 – 13.3  $\text{g COD} \cdot \text{g}^{-1} \text{vs}$ ) were reported as optimum in hydrogen-  
10 producing systems (Basak et al., 2018; Ferraz Júnior et al., 2015a). The differences in  
11 the optimum F/M ratio in the literature can be attributed to the differences in the waste-  
12 type and composition as well as the anaerobic sludges.

### 13 **3.5. Kinetic analyses of hydrogen production**

14 Kinetics parameters can also describe the performance of processes. Modified  
15 Gompertz model was used to describe the best condition for producing hydrogen (S.no.  
16 6; Table 2), considering the co-fermentation of CW and YMW. Concomitantly, the  
17 S.no. 12 represented the condition where the CW was used as only substrate for same  
18 purpose. To compare such behaviour between samples, it was assumed: (i) no influence  
19 of pH as previous discussed (*subhead 3.2.*) and (ii) low value for the F/M ratio  
20 (1.8 – 2.3  $\text{g COD} \cdot \text{g}^{-1} \text{vs}$ ). The Modified Gompertz model was found to describe the  
21 experimental data at an excellent level ( $R^2 > 0.990$ ) for both assays. The co-  
22 fermentation process improved the accumulated hydrogen production ( $\text{AcH}_2\text{P}$ ) and rate  
23 (R) in up to 4.5 and 7.5 folds, respectively, compared to the condition without YMW  
24 (Figure 2) (Table 6). However, the addition of YMW delayed the lag phase by 4.5 hours  
25 while, in its absence, hydrogen production occurred immediately (Table 5). It is worth  
26 mentioning that, after biogas being washed in NaOH solution (12% w/v), the hydrogen  
27 content was superior to 99% in all reactors throughout the experiment.

28

29 **[Figure 2]**

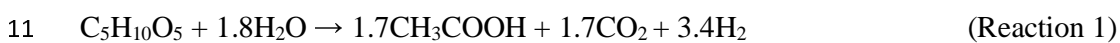
30

31 **[Table 6]**

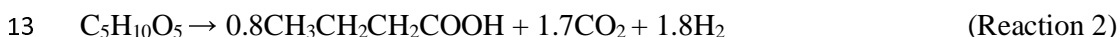
### 1       **3.6. Short and medium-organic acids: precursor and non-precursor of** 2       **hydrogen**

3       The total reducing sugars (TRS) in the medium source is mainly composed of glucose,  
4       lactose, xylose and arabinose, as depicted in Castelló et al., (2019) and Ferraz Júnior et  
5       al., (2020). However, the batch reactor “S. no. 12” presents only hexoses in the liquid  
6       medium, considering the absence of YM in the experiment. The TRS presented an  
7       average value of conversion of 93.4% suggesting that the organic compost provided a  
8       microbial community able to consume both pentoses and hexoses (Reactions 1-4)  
9       (Tabassum et al., 2017; Xia et al., 2015).

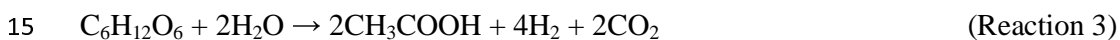
10      *Pentose conversion to acetate*



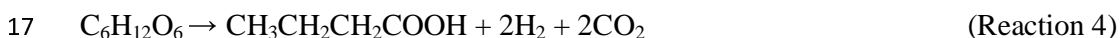
12      *Pentose conversion to butyrate*



14      *Hexose conversion to acetate*

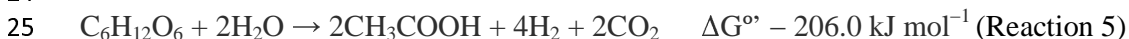


16      *Hexose conversion to butyrate*

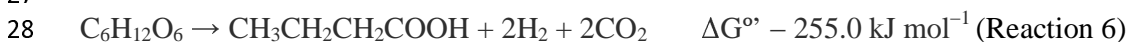


18      The main metabolites observed were butyrate (114-132 mM), lactate (109-140 mM)  
19      followed by acetate (16-109 mM) and ethanol (8-74 mM) (Figure 3A). As widely  
20      known, acetate-type fermentation from glucose results in  $4 \text{ molH}_2 \cdot \text{mol}^{-1}_{\text{glucose}}$  (Reaction  
21      5). Similarly, butyrate- and ethanol-type fermentations lead to a yield of only 2  
22       $\text{molH}_2 \cdot \text{mol}^{-1}_{\text{glucose}}$  (Reaction 6-7) (Toledo-Alarcón et al., 2018).

23      *Acetate-type fermentation*



26      *Butyrate-type fermentation*



29      *Ethanol-type fermentation (glucose into ethanol and acetate)*



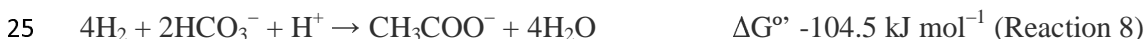
2  $\Delta G^{\circ} = -205.2 \text{ kJ mol}^{-1}$  (Reaction 7)

3 The above reactions give the impression that higher values for acetate are directly  
4 related to higher hydrogen production. However, acetate is also a product of hydrogen  
5 consumers (homoacetogens) whereas butyrate is inexorably linked to hydrogen-  
6 producing in mixed culture, and no direct hydrogen consumption pathway related to  
7 butyrate production has been reported so far (Guo et al., 2014). Furthermore, butyrate  
8 formation reaction is more energetically favorable, considering the Gibb's free energy  
9 (Reaction 6). In turn, ethanol-type fermentation occurs in condition with high acetate  
10 concentration and low pH (lower than 4) (Mota et al., 2018).

11 The theoretical hydrogen production was calculated for each batch reactor. The  
12 measured hydrogen ranged between 6.3% and 41.6% of the theoretical hydrogen  
13 computed, suggesting homoacetogenesis play a key role in all batch reactors (Reaction  
14 8). This finding is corroborated by the estimation of the measured acetate from  
15 homoacetogenesis (Equation 8). Acetate issued by such a pathway reached values up to  
16 94.6% which explains the “low values” of hydrogen production and supports the  
17 butyrate-type fermentation as the main hydrogen-producing pathway in this study.

18 The increment of agitation speed might be a strategy to avoid hydrogen consumption by  
19 homoacetogens (Montiel Corona et al., 2018). These authors observed a depletion of  
20 9% in homoacetogenesis after increasing the agitation speed. Alternatively, biogas  
21 sequestration from the headspace of a fermentative system was able to lower the  
22 availability of hydrogen in the liquid medium and, thus, minimizing homoacetogens  
23 (Ferraz Júnior et al., 2020).

24 *Homoacetogenesis (the Wood–Ljungdahl pathway)*



26 Residual sugars, hydrogen production and metabolites represented between and 70.2%  
27 and 83.8% of the COD fed to batch reactors. The organic matter conversion into  
28 biomass was not computed (Supplementary Table 1).

29 The experiments performed give also suitable information about the production of  
30 lactate, an added-value compound used to produce poly-lactic acid, a biodegradable  
31 plastic (Parra-Ramírez et al., 2019) and, interestingly, caproate, a medium-chain organic

1 acid used as feed additive, plant growth promoter, etc. (Pan et al., 2020). Lactate is  
2 often reported in mesophilic hydrogen producing systems as an inhibitor of biohydrogen  
3 production process and rarely discussed as a commercial product (Reaction 9). In this  
4 study, high values of lactate (~ 140 mM) were obtained at different values of pH (5.9,  
5 8.5 and 11.0) of co-fermentation process (Table 3A). Lactate production, separation and  
6 purification was economically viable for some of the scales evaluated at a value of 1.89  
7 USD.kg<sup>-1</sup> (Parra-Ramírez et al., 2019). Yet, lactate jointly with ethanol are reported as  
8 ideal substrates for supplying electrons during carboxylic acid chain elongation through  
9 the reverse β-oxidation (RBO) reaction (Barker and Taha, 1942) (Reactions 10-11). In  
10 this process, the sequential formation of butyrate and, then, caproate from acetate is  
11 possible (Cavalcante et al., 2017). The maximum caproate production observed was ~  
12 45 mM at pH 8.5 of the CW and YMW dark fermentation (Table 3A). Its production  
13 probably occurred in two steps: (i) fermentation of organic matter and hydrogen  
14 consumption to acetate production via the *Wood-Ljungdahl* pathway followed by (ii)  
15 the RBO pathway. Furthermore, the market price of caproate is more than 10 times  
16 higher than that of ethanol (Cavalcante et al., 2017). Despite these high values of short-  
17 and medium-chain organic acids production here observed, more detailed research on  
18 this topic must be performed in order to optimize the process, considering their  
19 productivity and yield.

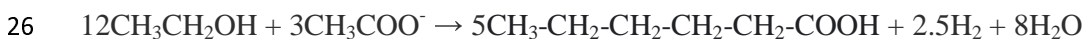
20 *Lactic-type fermentation (glucose into lactate and ethanol)*



22 *Overall production of n-caproate from lactate*



25 *Overall production of n-caproate from ethanol and acetate*



### 28 **3.7. Taxonomic profile of the microbial community in the co-fermentation** 29 **batch reactors**

30 16S ribosomal RNA gene sequences were analyzed to characterize the microbial  
31 community structure and reveal the CW and YMW co-fermentation conditions-



1 associated changes (Figure 3B). According to the results, the most abundant  
2 microorganisms detected in the co-fermentation process were related to the following  
3 roles: (i) hydrogen production (*Alkaliphilus*, *Bacillus*, *Clostridium*, *Romboutsia*,  
4 *Ruminiclostridium* and *Sporacetigenium*) ( Ferraz Júnior et al., 2013, 2014, 2015a,  
5 2015b, An et al., 2018, An et al., 2020, Bu et al., 2021) (ii) ethanol-hydrogen co-  
6 production (*Hydrogenispora*) (Liu et al., 2014); (iii) hydrogen consumption (*Oxobacter*)  
7 (Greening et al., 2019); (iv) lactate production (*Enterococcus*, *Lactobacillus*,  
8 *Lactococcus*, *Leuconostoc*, *Romboutsia*, *Sporolactobacillus* and *Streptococcus*)  
9 (Castelló et al., 2020; Ferraz Júnior et al., 2017; Fuess et al., 2018) and (v) caproate  
10 production (*Caproiciproducens*) (Kim et al., 2015). These microorganisms are  
11 consistent with fermentative systems studies and coherently related to the metabolites  
12 presented in Figure 3A and discussed in subhead 3.6.

13 To further understand the interaction among the indicators of batch-reactor  
14 performances, a Principal Component Analysis (PCA) was performed (Figure 4). Two  
15 principal components accounted for nearly 45% of the dataset variance. The results  
16 showed two well-defined axes or principal components (PC): PC 1 which represents the  
17 main effect of lactate and its producers' microorganisms opposing to H<sub>2</sub>Y, acetate and  
18 butyrate as well as caproate and *Caproiciproducens* (PC 2). These findings reinforcing  
19 that acetate-, butyrate-, caproate- and lactate-type fermentation were the main metabolic  
20 pathways (*subhead 3.6*) observed from the CCD experiments. The results also showed a  
21 low variation of ethanol and propionate, considering the variables and their levels  
22 studied. Finally, it should be noticed that the variables YMW, pH and inoculum were  
23 computed in the PCA as supplementary elements. It means that such coordinates are  
24 predicted using only the information provided by the performed PCA on active  
25 variables/individuals.

26

27

### [Table S1]

28 Linked to Ferraz Júnior et al. (2014b), Ferraz Júnior et al. (2014b) and Luo et al. (Luo et al., 2011).

29

### [Figure 4 – Please here]

## 30 4. Conclusions

31 Co-fermentation of cheese whey and alkaline-pretreated Yerba Mate waste can be  
32 potentially used to produce hydrogen and short- and medium-chain organic acids. In

1 terms of hydrogen production, the increase of inoculum and YMW concentrations had  
2 positive effects in the process while the initial pH had no significant effect on it,  
3 considering the conditions evaluated. Butyrate-type fermentation was the main  
4 hydrogen-producing pathway. Acetate from homoacetogenesis was accounted for all  
5 conditions evaluated. The Central Composite Design also indicated operating conditions  
6 to produce moderate-to-high concentrations of added value compounds, for instance,  
7 butyrate, lactate and caproate. 16S ribosomal DNA gene sequences analysis revealed  
8 five groups of microorganisms related to hydrogen, lactate and caproate production,  
9 ethanol-hydrogen co-production and hydrogen consumption. Principal Component  
10 Analysis computed three well-defined groups related to the hydrogen, lactate and  
11 caproate production.

### 12 *Acknowledgements*

13 The authors gratefully acknowledge support of the Clemente Estable Institute of  
14 Biological Research (IIBCE), the Program of Basic Science Development of Uruguay  
15 (PEDECIBA-Chemistry), the Uruguayan National System of Researchers and National  
16 Agency for Research and Innovation (SNI-ANII).

17

### 18 *Declaration of Competing Interest*

19 The authors declare that they have no known competing financial interests or personal  
20 relationships that could have appeared to influence the work reported in this paper.

### 21 **References**

- 22 Adorno, M.A.T., Hirasawa, J.S., Varesche, M.B.A., 2014. Development and Validation  
23 of Two Methods to Quantify Volatile Acids (C2-C6) by GC/FID: Headspace  
24 (Automatic and Manual) and Liquid-Liquid Extraction (LLE). *Am. J. Anal. Chem.*  
25 05, 406–414. <https://doi.org/10.4236/ajac.2014.57049>
- 26 Akhlaghi, M., Boni, M.R., De Gioannis, G., Muntoni, A., Poletini, A., Pomi, R., Rossi,  
27 A., Spiga, D., 2017. A parametric response surface study of fermentative hydrogen  
28 production from cheese whey. *Bioresour. Technol.* 244, 473–483.  
29 <https://doi.org/10.1016/j.biortech.2017.07.158>
- 30 An, Q., Cheng, J.-R., Wang, Y.-T., Zhu, M.-J., 2020. Performance and energy recovery

- 1 of single and two stage biogas production from paper sludge: *Clostridium*  
2 *thermocellum* augmentation and microbial community analysis. *Renew. Energy*  
3 148, 214–222. <https://doi.org/10.1016/j.renene.2019.11.142>
- 4 An, Q., Wang, J.-L., Wang, Y.-T., Lin, Z.-L., Zhu, M.-J., 2018. Investigation on  
5 hydrogen production from paper sludge without inoculation and its enhancement  
6 by *Clostridium thermocellum*. *Bioresour. Technol.* 263, 120–127.  
7 <https://doi.org/10.1016/j.biortech.2018.04.105>
- 8 APHA, 2005. Standard methods for the examination of water and wastewater, 21<sup>st</sup> ed.  
9 American Public Health Association, Washington, DC, New York: American  
10 Public Health Association.
- 11 Barker, H.A., Taha, S.M., 1942. *Clostridium kluyverii*, an Organism Concerned in the  
12 Formation of Caproic Acid from Ethyl Alcohol. *J. Bacteriol.* 43, 347–63.  
13 <https://doi.org/10.1128/JB.43.3.347-363.1942>
- 14 Basak, B., Fatima, A., Jeon, B.-H., Ganguly, A., Chatterjee, P.K., Dey, A., 2018.  
15 Process kinetic studies of biohydrogen production by co-fermentation of fruit-  
16 vegetable wastes and cottage cheese whey. *Energy Sustain. Dev.* 47, 39–52.  
17 <https://doi.org/10.1016/j.esd.2018.08.004>
- 18 Bina, B., Amin, M.M., Pourzamani, H., Fatehizadeh, A., Ghasemian, M., Mahdavi, M.,  
19 Taheri, E., 2019. Biohydrogen production from alkaline wastewater: The  
20 stoichiometric reactions, modeling, and electron equivalent. *MethodsX* 6, 1496–  
21 1505. <https://doi.org/10.1016/j.mex.2019.06.013>
- 22 Borin, G.P., Alves, R.F., Ferraz Júnior, A.D.N., 2019. Current Status of  
23 Biotechnological Processes in the Biofuel Industries, in: *Bioprocessing for*  
24 *Biomolecules Production*. John Wiley & Sons, Ltd, Chichester, UK, pp. 47–69.  
25 <https://doi.org/10.1002/9781119434436.ch3>
- 26 Borshchevskaya, L.N., Gordeeva, T.L., Kalinina, A.N., Sineokii, S.P., 2016.  
27 Spectrophotometric determination of lactic acid. *J. Anal. Chem.* 71, 755–758.  
28 <https://doi.org/10.1134/S1061934816080037>
- 29 Box G.E, Wilson, K., 1951. On the Experimental Attainment of Optimum Conditions.  
30 *J. R. Stat. Soc.* 13, 1–45.

- 1 Bu, J., Wang, Y.-T., Deng, M.-C., Zhu, M.-J., 2021. Enhanced enzymatic hydrolysis  
2 and hydrogen production of sugarcane bagasse pretreated by peroxyformic acid.  
3 *Bioresour. Technol.* 326, 124751. <https://doi.org/10.1016/j.biortech.2021.124751>
- 4 Caporaso, J.G., Lauber, C.L., Walters, W. a, Berg-Lyons, D., Huntley, J., Fierer, N.,  
5 Owens, S.M., Betley, J., Fraser, L., Bauer, M., Gormley, N., Gilbert, J. a, Smith,  
6 G., Knight, R., 2012. Ultra-high-throughput microbial community analysis on the  
7 Illumina HiSeq and MiSeq platforms. *ISME J.* 6, 1621–1624.  
8 <https://doi.org/10.1038/ismej.2012.8>
- 9 Caporaso, J.G., Lauber, C.L., Walters, W.A., Berg-Lyons, D., Lozupone, C.A.,  
10 Turnbaugh, P.J., Fierer, N., Knight, R., 2011. Global patterns of 16S rRNA  
11 diversity at a depth of millions of sequences per sample. *Proc. Natl. Acad. Sci. U.*  
12 *S. A.* 108 Suppl, 4516–22. <https://doi.org/10.1073/pnas.1000080107>
- 13 Castelló, E., Nunes Ferraz-Junior, A.D., Andreani, C., Anzola-Rojas, M. del P.,  
14 Borzacconi, L., Buitrón, G., Carrillo-Reyes, J., Gomes, S.D., Maintinguer, S.I.,  
15 Moreno-Andrade, I., Palomo-Briones, R., Razo-Flores, E., Schiappacasse-Dasati,  
16 M., Tapia-Venegas, E., Valdez-Vázquez, I., Vesga-Baron, A., Zaiat, M.,  
17 Etchebehere, C., 2020. Stability problems in the hydrogen production by dark  
18 fermentation: Possible causes and solutions. *Renew. Sustain. Energy Rev.* 119,  
19 109602. <https://doi.org/10.1016/j.rser.2019.109602>
- 20 Cavalcante, W. de A., Leitão, R.C., Gehring, T.A., Angenent, L.T., Santaella, S.T.,  
21 2017. Anaerobic fermentation for n-caproic acid production: A review. *Process*  
22 *Biochem.* 54, 106–119. <https://doi.org/10.1016/j.procbio.2016.12.024>
- 23 Chen, S., Song, L., Dong, X., 2006. *Sporacetigenium mesophilum* gen. nov., sp. nov.,  
24 isolated from an anaerobic digester treating municipal solid waste and sewage. *Int.*  
25 *J. Syst. Evol. Microbiol.* 56, 721–725. <https://doi.org/10.1099/ijs.0.63686-0>
- 26 Claesson, M.J., O’Sullivan, O., Wang, Q., Nikkilä, J., Marchesi, J.R., Smidt, H., de  
27 Vos, W.M., Ross, R.P., O’Toole, P.W., 2009. Comparative Analysis of  
28 Pyrosequencing and a Phylogenetic Microarray for Exploring Microbial  
29 Community Structures in the Human Distal Intestine. *PLoS One* 4, e6669.  
30 <https://doi.org/10.1371/journal.pone.0006669>
- 31 Dareioti, M.A., Vavouraki, A.I., Kornaros, M., 2014. Effect of pH on the anaerobic

- 1 acidogenesis of agroindustrial wastewaters for maximization of bio-hydrogen  
2 production: A lab-scale evaluation using batch tests. *Bioresour. Technol.* 162, 218–  
3 227. <https://doi.org/10.1016/j.biortech.2014.03.149>
- 4 Edgar, R.C., Haas, B.J., Clemente, J.C., Quince, C., Knight, R., 2011. UCHIME  
5 improves sensitivity and speed of chimera detection. *Bioinformatics* 27, 2194–  
6 2200. <https://doi.org/10.1093/bioinformatics/btr381>
- 7 Fernández, C., Carracedo, B., Martínez, E.J., Gómez, X., Morán, A., 2014. Application  
8 of a packed bed reactor for the production of hydrogen from cheese whey  
9 permeate: Effect of organic loading rate. *J. Environ. Sci. Heal. Part A* 49, 210–217.  
10 <https://doi.org/10.1080/10934529.2013.838885>
- 11 Ferraz-Júnior; Antônio Djalma Nunes, Etchelet, M.I., Braga, A.F.M., Clavijo, L.,  
12 Loaces, I., Noya, F., Etchebehere, C., 2020. Alkaline pretreatment of yerba mate  
13 (*Ilex paraguariensis*) waste for unlocking low-cost cellulosic biofuel. *Fuel* 266,  
14 117068. <https://doi.org/10.1016/j.fuel.2020.117068>
- 15 Ferraz Júnior, A.D.N., 2013. Digestão anaeróbia da vinhaça da cana de açúcar em reator  
16 acidogênico de leito fixo seguido de reator metanogênico de manta de lodo.  
17 Universidade de São Paulo, São Carlos. [https://doi.org/10.11606/T.18.2013.tde-  
18 27082014-092345](https://doi.org/10.11606/T.18.2013.tde-27082014-092345)
- 19 Ferraz Júnior, A.D.N., Damásio, A.R.L., Paixão, D.A.A., Alvarez, T.M., Squina, F.M.,  
20 2017. Applied Metagenomics for Biofuel Development and Environmental  
21 Sustainability, in: *Advances of Basic Science for Second Generation Bioethanol*  
22 *from Sugarcane*. Springer International Publishing, Cham, pp. 107–129.  
23 [https://doi.org/10.1007/978-3-319-49826-3\\_7](https://doi.org/10.1007/978-3-319-49826-3_7)
- 24 Ferraz Júnior, A.D.N., Etchebehere, C., Zaiat, M., 2015a. High organic loading rate on  
25 thermophilic hydrogen production and metagenomic study at an anaerobic packed-  
26 bed reactor treating a residual liquid stream of a Brazilian biorefinery. *Bioresour.*  
27 *Technol.* 186, 81–88. <https://doi.org/10.1016/j.biortech.2015.03.035>
- 28 Ferraz Júnior, A.D.N., Etchebehere, C., Zaiat, M., 2015b. Mesophilic hydrogen  
29 production in acidogenic packed-bed reactors (apbr) using raw sugarcane vinasse  
30 as substrate: Influence of support materials. *Anaerobe*.  
31 <https://doi.org/10.1016/j.anaerobe.2015.04.008>

- 1 Ferraz Júnior, A.D.N., Pages, C., Latrille, E., Bernet, N., Zaiat, M., Trably, E., 2020.  
2 Biogas sequestration from the headspace of a fermentative system enhances  
3 hydrogen production rate and yield. *Int. J. Hydrogen Energy*.  
4 <https://doi.org/10.1016/j.ijhydene.2020.02.064>
- 5 Ferraz Júnior, A.D.N., Wenzel, J., Etchebehere, C., Zaiat, M., 2014a. Effect of organic  
6 loading rate on hydrogen production from sugarcane vinasse in thermophilic  
7 acidogenic packed bed reactors. *Int. J. Hydrogen Energy* 39, 16852–16862.  
8 <https://doi.org/10.1016/j.ijhydene.2014.08.017>
- 9 Ferraz Júnior, A.D.N., Zaiat, M., Gupta, M., Elbeshbishy, E., Hafez, H., Nakhla, G.,  
10 2014b. Impact of organic loading rate on biohydrogen production in an up-flow  
11 anaerobic packed bed reactor (UAnPBR). *Bioresour. Technol.* 164, 371–9.  
12 <https://doi.org/10.1016/j.biortech.2014.05.011>
- 13 Fuess, L.T., Ferraz, A.D.N., Machado, C.B., Zaiat, M., 2018. Temporal dynamics and  
14 metabolic correlation between lactate-producing and hydrogen-producing bacteria  
15 in sugarcane vinasse dark fermentation: The key role of lactate. *Bioresour.*  
16 *Technol.* 247, 426–433. <https://doi.org/10.1016/j.biortech.2017.09.121>
- 17 Greening, C., Geier, R., Wang, C., Woods, L.C., Morales, S.E., McDonald, M.J.,  
18 Rushton-Green, R., Morgan, X.C., Koike, S., Leahy, S.C., Kelly, W.J., Cann, I.,  
19 Attwood, G.T., Cook, G.M., Mackie, R.I., 2019. Diverse hydrogen production and  
20 consumption pathways influence methane production in ruminants. *ISME J.* 13,  
21 2617–2632. <https://doi.org/10.1038/s41396-019-0464-2>
- 22 Grosser, A., Neczaj, E., 2018. Sewage sludge and fat rich materials co-digestion -  
23 Performance and energy potential. *J. Clean. Prod.* 198, 1076–1089.  
24 <https://doi.org/10.1016/j.jclepro.2018.07.124>
- 25 Guo, X.M., Trably, E., Latrille, E., Carrere, H., Steyer, J.-P., 2014. Predictive and  
26 explicative models of fermentative hydrogen production from solid organic waste:  
27 Role of butyrate and lactate pathways. *Int. J. Hydrogen Energy* 39, 7476–7485.  
28 <https://doi.org/10.1016/j.ijhydene.2013.08.079>
- 29 Kim, B.-C., Seung Jeon, B., Kim, S., Kim, H., Um, Y., Sang, B.-I., 2015.  
30 *Caproiciproducens galactitolivorans* gen. nov., sp. nov., a bacterium capable of  
31 producing caproic acid from galactitol, isolated from a wastewater treatment plant.

- 1 Int. J. Syst. Evol. Microbiol. 65, 4902–4908.  
2 <https://doi.org/10.1099/ijsem.0.000665>
- 3 Kim, D.-H., Kim, S.-H., Jung, K.-W., Kim, M.-S., Shin, H.-S., 2011. Effect of initial pH  
4 independent of operational pH on hydrogen fermentation of food waste. *Bioresour.*  
5 *Technol.* 102, 8646–8652. <https://doi.org/10.1016/j.biortech.2011.03.030>
- 6 Koyama, M.H., Messias, M., Junior, A., Zaiat, M., 2016. Kinetics of thermophilic  
7 acidogenesis of typical Brazilian sugarcane vinasse. *Energy* 116, 1097–1103.  
8 <https://doi.org/10.1016/j.energy.2016.10.043>
- 9 Lee, Z.-K., Li, S.-L., Lin, J.-S., Wang, Y.-H., Kuo, P.-C., Cheng, S.-S., 2008. Effect of  
10 pH in fermentation of vegetable kitchen wastes on hydrogen production under a  
11 thermophilic condition. *Int. J. Hydrogen Energy* 33, 5234–5241.  
12 <https://doi.org/10.1016/j.ijhydene.2008.05.006>
- 13 Levin, D.B., Pitt, L., Love, M., 2004. Biohydrogen production □: prospects and  
14 limitations to practical application 29, 173–185. [https://doi.org/10.1016/S0360-](https://doi.org/10.1016/S0360-3199(03)00094-6)  
15 [3199\(03\)00094-6](https://doi.org/10.1016/S0360-3199(03)00094-6)
- 16 Li, X., Guo, L., Liu, Y., Wang, Y., She, Z., Gao, M., Zhao, Y., 2020. Effect of salinity  
17 and pH on dark fermentation with thermophilic bacteria pretreated swine  
18 wastewater. *J. Environ. Manage.* 271, 111023.  
19 <https://doi.org/10.1016/j.jenvman.2020.111023>
- 20 Liu, Y., 1996. Bioenergetic interpretation on the S<sub>0</sub>X<sub>0</sub> ratio in substrate-sufficient batch  
21 culture. *Water Res.* 30, 2766–2770. [https://doi.org/10.1016/S0043-1354\(96\)00157-](https://doi.org/10.1016/S0043-1354(96)00157-1)  
22 [1](https://doi.org/10.1016/S0043-1354(96)00157-1)
- 23 Liu, Y., Qiao, J.-T., Yuan, X.-Z., Guo, R.-B., Qiu, Y.-L., 2014. *Hydrogenispora*  
24 *ethanolica* gen. nov., sp. nov., an anaerobic carbohydrate-fermenting bacterium  
25 from anaerobic sludge. *Int. J. Syst. Evol. Microbiol.* 64, 1756–1762.  
26 <https://doi.org/10.1099/ijs.0.060186-0>
- 27 Lovato, G., Albanez, R., Stracieri, L., Ruggero, L.S., Ratusznei, S.M., Rodrigues,  
28 J.A.D., 2018. Hydrogen production by co-digesting cheese whey and glycerin in an  
29 AnSBBR: Temperature effect. *Biochem. Eng. J.* 138, 81–90.  
30 <https://doi.org/10.1016/j.bej.2018.07.007>

- 1 Lovato, G., Augusto, I.M.G., Ferraz Júnior, A.D.N., Albanez, R., Ratusznei, S.M.,  
2 Etchebehere, C., Zaiat, M., Rodrigues, J.A.D., 2021. Reactor start-up strategy as  
3 key for high and stable hydrogen production from cheese whey thermophilic dark  
4 fermentation. *Int. J. Hydrogen Energy*.  
5 <https://doi.org/10.1016/j.ijhydene.2021.06.010>
- 6 Lucas, S.D.M., Peixoto, G., Mockaitis, G., Zaiat, M., Gomes, S.D., 2015. Energy  
7 recovery from agro-industrial wastewaters through biohydrogen production:  
8 Kinetic evaluation and technological feasibility. *Renew. Energy* 75, 496–504.  
9 <https://doi.org/10.1016/j.renene.2014.10.025>
- 10 Luo, G., Karakashev, D., Xie, L., Zhou, Q., Angelidaki, I., 2011. Long-term effect of  
11 inoculum pretreatment on fermentative hydrogen production by repeated batch  
12 cultivations: Homoacetogenesis and methanogenesis as competitors to hydrogen  
13 production. *Biotechnol. Bioeng.* 108, 1816–1827. <https://doi.org/10.1002/bit.23122>
- 14 Luongo, V., Policastro, G., Ghimire, A., Pirozzi, F., Fabbricino, M., 2019. Repeated-  
15 Batch Fermentation of Cheese Whey for Semi-Continuous Lactic Acid Production  
16 Using Mixed Cultures at Uncontrolled pH. *Sustainability* 11, 3330.  
17 <https://doi.org/10.3390/su11123330>
- 18 Marone, A., Varrone, C., Fiocchetti, F., Giussani, B., Izzo, G., Mentuccia, L., Rosa, S.,  
19 Signorini, A., 2015. Optimization of substrate composition for biohydrogen  
20 production from buffalo slurry co-fermented with cheese whey and crude glycerol,  
21 using microbial mixed culture. *Int. J. Hydrogen Energy* 40, 209–218.  
22 <https://doi.org/10.1016/j.ijhydene.2014.11.008>
- 23 Miller, G.L., 1959. Use of Dinitrosalicylic Acid Reagent for Determination of Reducing  
24 Sugar. *Anal. Chem.* 31, 426–428. <https://doi.org/10.1021/ac60147a030>
- 25 Mohd Yasin, N.H., Rahman, N.A., Man, H.C., Mohd Yusoff, M.Z., Hassan, M.A.,  
26 2011. Microbial characterization of hydrogen-producing bacteria in fermented food  
27 waste at different pH values. *Int. J. Hydrogen Energy* 36, 9571–9580.  
28 <https://doi.org/10.1016/j.ijhydene.2011.05.048>
- 29 Montiel Corona, V., Razo-Flores, E., Corona, Elías; Razo-Flores, V., 2018. Continuous  
30 hydrogen and methane production from Agave tequilana bagasse hydrolysate by  
31 sequential processes to maximize energy recovery efficiency. *Bioresour. Technol.*



- 1           249, 334–341. <https://doi.org/10.1016/j.biortech.2017.10.032>
- 2   Mota, V.T., Ferraz Júnior, A.D.N., Trably, E., Zaiat, M., 2018. Biohydrogen production  
3           at pH below 3.0: Is it possible? *Water Res.* 128.  
4           <https://doi.org/10.1016/j.watres.2017.10.060>
- 5   Pan, X.-R., Huang, L., Fu, X.-Z., Yuan, Y.-R., Liu, H.-Q., Li, W.-W., Yu, L., Zhao, Q.-  
6           B., Zuo, J., Chen, L., Lam, P.K.-S., 2020. Long-term, selective production of  
7           caproate in an anaerobic membrane bioreactor. *Bioresour. Technol.* 302, 122865.  
8           <https://doi.org/10.1016/j.biortech.2020.122865>
- 9   Parra-Ramírez, D., Martínez, A., Cardona, C.A., 2019. Lactic acid production from  
10           glucose and xylose using the lactogenic *Escherichia coli* strain JU15: Experiments  
11           and techno-economic results. *Bioresour. Technol.* 273, 86–92.  
12           <https://doi.org/10.1016/j.biortech.2018.10.061>
- 13   Rao, R., Basak, N., 2021. Optimization and modelling of dark fermentative hydrogen  
14           production from cheese whey by *Enterobacter aerogenes* 2822. *Int. J. Hydrogen*  
15           *Energy* 46, 1777–1800. <https://doi.org/10.1016/j.ijhydene.2020.10.142>
- 16   Sun, C., Xia, A., Liao, Q., Fu, Q., Huang, Y., Zhu, X., Wei, P., Lin, R., Murphy, J.D.,  
17           2018. Improving production of volatile fatty acids and hydrogen from microalgae  
18           and rice residue: Effects of physicochemical characteristics and mix ratios. *Appl.*  
19           *Energy* 230, 1082–1092. <https://doi.org/10.1016/j.apenergy.2018.09.066>
- 20   Tabassum, M.R., Xia, A., Murphy, J.D., 2017. Potential of seaweed as a feedstock for  
21           renewable gaseous fuel production in Ireland. *Renew. Sustain. Energy Rev.* 68,  
22           136–146. <https://doi.org/10.1016/j.rser.2016.09.111>
- 23   Toledo-Alarcón, J., Capson-Tojo, G., Marone, A., Paillet, F., Ferraz Júnior, A.D.N.,  
24           Chatellard, L., Bernet, N., Trably, E., 2018. Basics of bio-hydrogen production by  
25           dark fermentation, *Green Energy and Technology*. [https://doi.org/10.1007/978-](https://doi.org/10.1007/978-981-10-7677-0_6)  
26           981-10-7677-0\_6
- 27   Xia, A., Cheng, J., Ding, L., Lin, R., Song, W., Su, H., Zhou, J., Cen, K., 2015.  
28           Substrate consumption and hydrogen production via co-fermentation of monomers  
29           derived from carbohydrates and proteins in biomass wastes. *Appl. Energy* 139, 9–  
30           16. <https://doi.org/10.1016/j.apenergy.2014.11.016>

- 1 Xia, A., Jacob, A., Tabassum, M.R., Herrmann, C., Murphy, J.D., 2016. Production of  
2 hydrogen, ethanol and volatile fatty acids through co-fermentation of macro- and  
3 micro-algae. *Bioresour. Technol.* 205, 118–125.  
4 <https://doi.org/10.1016/j.biortech.2016.01.025>
- 5 Yang, G., Hu, Y., Wang, J., 2019. Biohydrogen production from co-fermentation of  
6 fallen leaves and sewage sludge. *Bioresour. Technol.* 285, 121342.  
7 <https://doi.org/10.1016/j.biortech.2019.121342>
- 8 Yin, Y., Chen, Y., Wang, J., 2021. Co-fermentation of sewage sludge and algae and  
9 Fe<sup>2+</sup> addition for enhancing hydrogen production. *Int. J. Hydrogen Energy* 46,  
10 8950–8960. <https://doi.org/10.1016/j.ijhydene.2021.01.009>

11

12

13

14

15

16

17

18

19

20

21

22

23

24

25

26 **Figure captions**

1 Figure 1. Response surface for the interactive effect on hydrogen yield ( $H_2Y$ ,  $MmH_2g^{-1}$   
2  $VS_{added}$ ) through co-fermentation process. Interactive effect of concentration of Yerba  
3 Mate waste and inoculum concentrations.

4

5 Figure 2. Cumulative hydrogen production (Observed) and unstructured mathematical  
6 model (Predicted) fit to the fermentative essays with (S.no. 6) and without (S.no. 12)  
7 YMW added.

8

9 Figure 3. A. Metabolites (organic acids and alcohols) of CCD experiments. B.  
10 Composition of microbial community at genus level of CCD experiments. Relative  
11 abundance above 1%.

12

13 Figure 4. Principal components analysis (PCA) of CCD experiments.

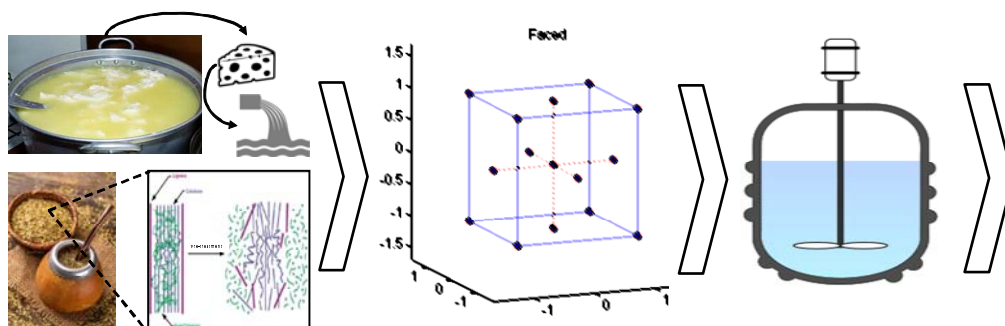
14

15

16

## Highlights

- Co-fermentation improved hydrogen production in up 7.5-folds compared to the sole CW-fed system.
- The initial pH had no effect on hydrogen-producing batch reactors.
- Hydrogen was produced as a coproduct to butyrate.
- Design of experiment indicated operating conditions to the production of lactate and caproate.



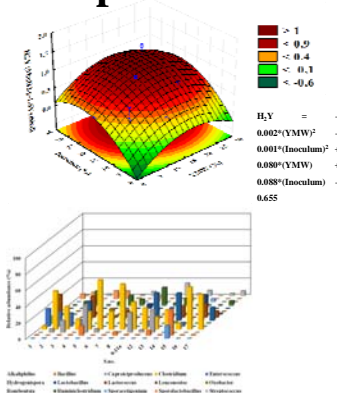
**Feedstock  
(CW + YMW)**

**Design of  
experiment**

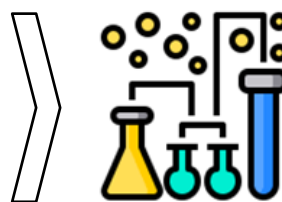
**Batch reactors**



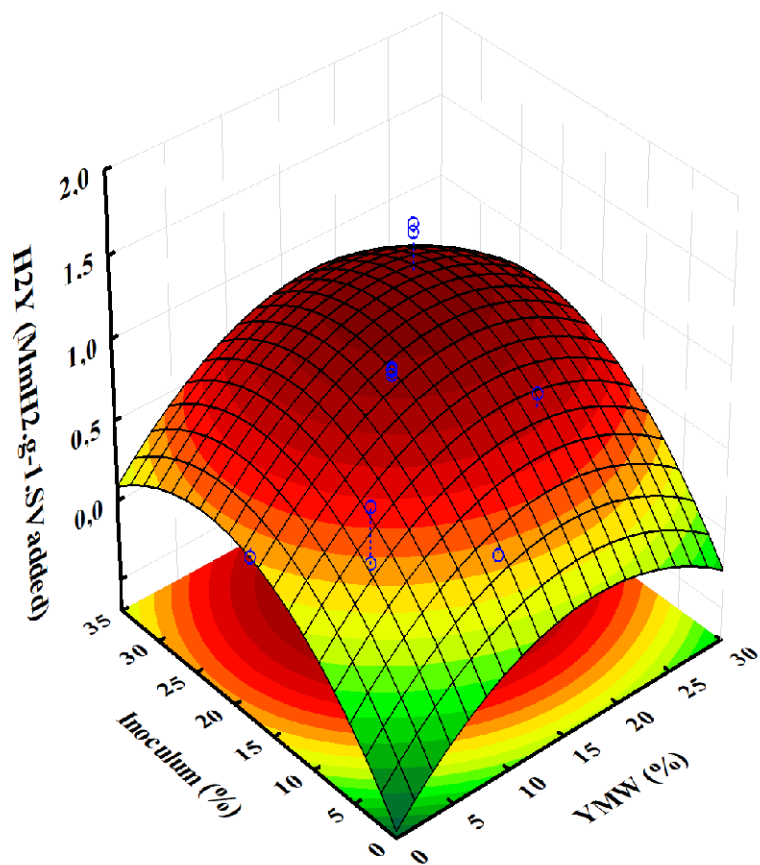
**BioH<sub>2</sub> and  
biocompounds  
production**

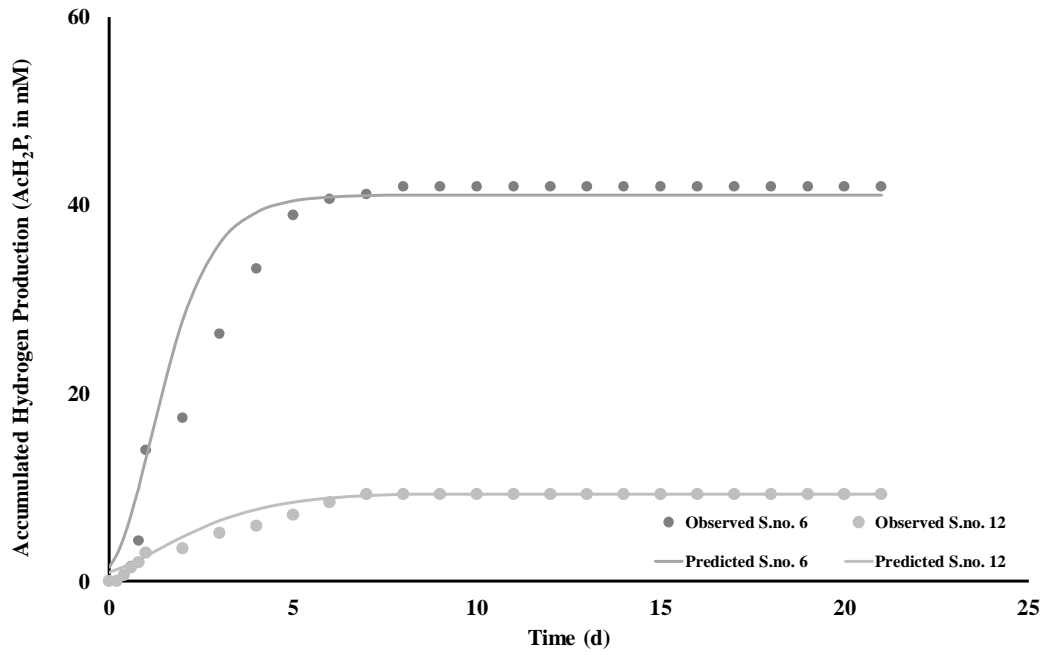


**Optimization of  
process**



**Optimized BioH<sub>2</sub>  
and biocompounds  
production**









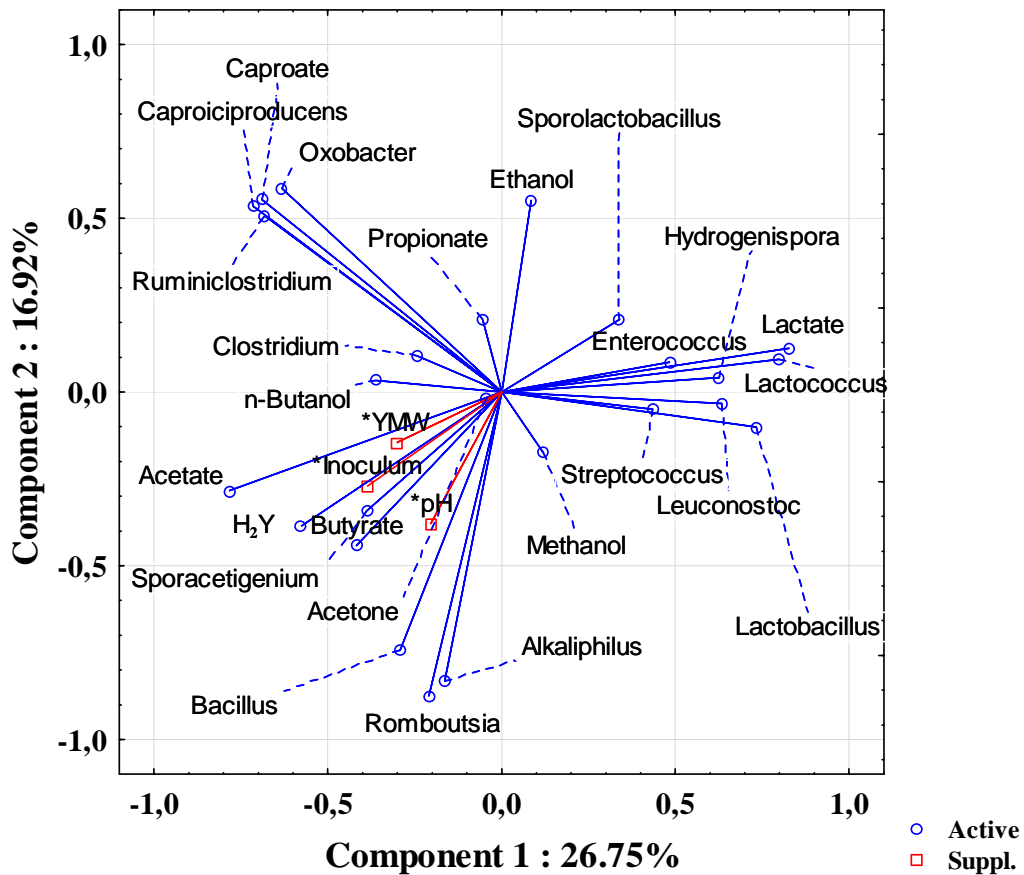


Table 1. Characterization of cheese whey (main substrate) and thermal-alkaline pretreated Yerba Mate waste (co-substrate).

<b>Variable</b>	<b>Unit</b>	<b>CW</b>	<b>Thermal-alkaline pretreated YMW</b>
pH	-	4.1±0.8	13.1±0.6
Total reducing sugars (TRS)	g.L <sup>-1</sup>	21.5	42.7
Total chemical oxygen demand (TCOD)	g-O <sub>2</sub> .L <sup>-1</sup>	50±2.5	135.0±6.9
Soluble chemical oxygen demand (SCOD)	g-O <sub>2</sub> .L <sup>-1</sup>	31.5±0.4	98.0±4.6
Total solids (TS)	gTS.L <sup>-1</sup>	33.2±0.6	101.7±2.8
Total volatile solids (TVS)	gTVS.L <sup>-1</sup>	31.0±0.8	50.2±3.3

Table 2. Three-variables design matrix for biohydrogen production from CW and YMW. Replications of center point or control are in bold.

S. no. <sup>a</sup>	Coded level			Uncoded level		
	X <sub>1</sub>	X <sub>2</sub>	X <sub>3</sub>	YMW <sup>b</sup>	pH	Inoculum <sup>c</sup>
1	-1	-1	-1	5.1	5.9	10.0
2	1	-1	-1	20.0	5.9	10.0
3	-1	1	-1	5.1	11.0	10.0
4	1	1	-1	20.0	11.0	10.0
5	-1	-1	1	5.1	5.9	25.0
6	1	-1	1	20.0	5.9	25.0
7	-1	1	1	5.1	11.0	25.0
8	1	1	1	20.0	11.0	25.0
<b>9</b>	0	0	0	12.5	8.5	17.5
<b>10</b>	0	0	0	12.5	8.5	17.5
<b>11</b>	0	0	0	12.5	8.5	17.5
12	- $\alpha$	0	0	0.0	8.5	17.5
13	$\alpha$	0	0	25.1	8.5	17.5
14	0	- $\alpha$	0	12.5	4.2	17.5
15	0	$\alpha$	0	12.5	12.7	17.5
16	0	0	- $\alpha$	12.5	8.5	4.9
17	0	0	$\alpha$	12.5	8.5	30.1

- The experiments were performed in a random order.
- Alkaline pretreated Yerba Mate Waste (YMW) in % w/w, as co-substrate.
- Inoculum, in % w/v (working volume of the reactor).

Table 3. Main results from the CCD experiments. Experimental (Y) and predicted ( $\hat{Y}$ ) values for the hydrogen yield ( $H_2Y$ , in  $mM-H_2 \cdot g^{-1} VS_{added}$ ) at 5% of significance. Replications of center point or control are in bold.

S. no. <sup>a</sup>	Uncoded level			$H_2Y$ ( $mM-H_2 \cdot g^{-1} VS_{added}$ )		Final pH
	YMW <sup>b</sup>	pH	Inoculum <sup>c</sup>	Y <sup>d</sup>	$\hat{Y}$ <sup>e</sup>	
1	5.1	5.9	10.0	0.36	0.40	3.4
2	20.0	5.9	10.0	0.58	0.58	3.4
3	5.1	11.0	10.0	0.72	0.69	4.5
4	20.0	11.0	10.0	0.63	0.57	3.7
5	5.1	5.9	25.0	0.58	0.55	4.9
6	20.0	5.9	25.0	1.35	1.28	4.5
7	5.1	11.0	25.0	0.84	0.75	4.9
8	20.0	11.0	25.0	1.30	1.17	5.2
<b>9</b>	<b>12.6</b>	<b>8.5</b>	<b>17.5</b>	<b>0.95</b>	<b>0.89</b>	4.1
<b>10</b>	<b>12.6</b>	<b>8.5</b>	<b>17.5</b>	<b>0.87</b>	<b>0.89</b>	4.2
<b>11</b>	<b>12.6</b>	<b>8.5</b>	<b>17.5</b>	<b>0.88</b>	<b>0.89</b>	4.1
12	0.0	8.5	17.5	0.31	0.33	3.5
13	25.1	8.5	17.5	0.73	0.84	4.9
14	12.6	4.2	17.5	0.98	0.97	3.6
15	12.6	12.7	17.5	0.99	1.13	5.3
16	12.6	8.5	4.9	0.33	0.32	3.5
17	12.6	8.5	30.1	0.81	0.95	4.9

a. Experiments were performed randomly. b. Alkaline pretreated Yerba Mate Waste (YMW) in % w/w, as co-substrate. c. Inoculum, in % w/v (working volume of the reactor). d. Experimental value. e. Predicted value.

Table 4. Maximum production and other parameters of BioH<sub>2</sub>, lactate and caproate production by mixed microbial cultures grown on different organic wastes.

Bioproduct	Reactor-type	Inoculum	Substrate	pH	Temp. (°C)	Maximum production (mM.L <sup>-1</sup> )	Maximum hydrogen yield (MmH <sub>2</sub> .g <sup>-1</sup> VS <sub>added</sub> )	Reference
<b>Hydrogen</b>	Batch	Acclimatized anaerobic sludge	Olive mill wastewater, cheese whey, cow manure	6.0	37	26.9	1.06	Dareioti et al., (2014)
	Batch	Thermal pretreatment poultry	Dairy wastewater	5.5	37	3.4	1.27	Lucas et al., (2015)
	Batch	Consortia from lagoon sediments	Buffalo slurry, cheese whey and crude glycerol	6.5	37	20.5	4.98	Marone et al., (2015)
	Batch	2-bromoethanesulfonate treated anaerobic sludge	Fruit vegetable waste, cottage cheese whey	7.0	37	118.1	5.69	Basak et al., (2018)
	Batch	Organic compost	Cheese whey and Yerba Mate	5.9 <sup>a</sup> (uncontrolled pH)	30	41.9	1.35	This study
<b>Lactate</b>	Continuous	Anaerobic sludge	Diluted whey	5.5	55	63.3	-	Choi et al., (2016)
	Semi-continuous	Thermal pretreatment anaerobic digestate	Cheese whey	6.0 – 4.5 (uncontrolled pH)	35	223.1	-	Luongo et al., (2019)
	Batch	Activated sludge	Potato peel waste	4.8 (uncontrolled pH)	35	163.2	-	Liang et al., (2014)
	Semi-continuous	Anaerobic sludge	Food waste	7.0 (uncontrolled pH)	35	206.5	-	Bonk et al., (2017)
	Batch	Organic compost	Cheese whey and Yerba Mate	5.9, 8.5 and 11.0 <sup>a</sup> (uncontrolled pH)	30	136.5 – 139.9	-	This study
<b>Caproate</b>	Batch	Mature pit mud	Strong-flavor liquor	~6.5	30	201.5	-	Zhu et al., (2015)
	Continuous	2-bromoethanesulfonate treated environmental sample	OFMSW <sup>b</sup> + ethanol	5.5	30	23.2	-	Grootscholten et al., (2013)
	Continuous	Acidogenic sludge	Lactic acid	5.5	34	27.7	-	Kucek et al., (2016)

Continuous	Acidogenic sludge	Synthetic wastewater (Acetate and ethanol)	5.5 (2.0 g-NaHCO <sub>3</sub> ·L <sup>-1</sup> )	30	22.6	-	Pan et al., (2020)
Batch	Organic compost	Cheese whey and Yerba Mate	8.5 <sup>a</sup> (uncontrolled pH)	30	44.0 – 47.0	-	This study

a. Initial value and uncontrolled pH. b. Organic fraction of municipal solid waste (OFMSW).

Table 5. Coefficients of fitted equation ( $Y = b_0 + b_1 X_1 + b_2 X_2 + b_3 X_3 + b_{12} X_1 X_2 + b_{13} X_1 X_3 + b_{23} X_2 X_3 + e$ ) and its percent significance.

<b>Coefficients</b>	
$b_0^a$	0.78
$b_1^a$	0.15
$b_2$	0.05
$b_3^a$	0.19
$b_{12}^a$	-0.08
$b_{13}^a$	0.14
$b_{23}$	-0.02
$e$	$\pm 0.01$
$p\text{-value}^{a, b}$	0.021
$p\text{-value}^c$	0.059
$R^2$	0.72

a. Significant at 5% level. b. Regression p-value. c. Residual p-value.

Table 6. Kinetic parameters estimated by Modified Gompertz model from batch-reactors with and without YMW added.

Parameters	Estimate <sup>a</sup>	Standard error <sup>a</sup>	LCL <sup>a, b</sup>	UCL <sup>a, c</sup>	R <sup>2</sup>
P (mM)	41.1 / 9.4	1.3 / 0.5	38.1 / 8.4	44.0 / 10.5	
R (mM.d <sup>-1</sup> )	16.2 / 2.1	2.2 / 0.3	11.3 / 1.5	21.1 / 2.6	0.992 / 0.990
$\lambda$ (d)	0.2 / -0.3	0.1 / 0.2	-0.1 / -0.8	0.5 / 0.2	

a. (S.no. 6: with YMW / S.no. 12: without YMW). b. Low-confidence limit. c. Up-confidence limit.